International Journal of Heat and Technology
Vol. 36, No. 4, December, 2018, pp. 1502-1509
Journal homepage: http://iieta.org/Journals/IJHT

Heat transfer measurement in rectangular channel with detach ribs by liquid crystal thermography

Sibendra Kumar Gharai*, Apurba Layek

Mechanical Engineering Department, NIT Durgapur 713209, India

Corresponding Author Email: skgharai@gmail.com

https://doi.org/10.18280/ijht.360444

Received: 27 March 2018
Accepted: 6 September 2018

Keywords:
aspect ratio, detach rib, liquid crystal thermography, relative roughness pitch, thermal performance parameter

ABSTRACT

Heat transfer is measured in a rectangular channel with detach transverse square ribs using liquid crystal thermography. The ribs were provided on one broad wall of rectangular duct of aspect ratio 4. The roughened surface was heated uniformly. The roughness parameters selected for this study were, relative roughness pitch (*P*/*e*) of values 7-11, clearance ratio (*C*/*e*) of values 0.37-0.57 and Reynolds number (Re) of values 8100-22300. The heat transfer coefficient has been compared with attached transverse square ribs at similar operating condition and result reveals that detach rib roughness is better than the attach ribs. It is observed that the thermal performance parameter increases with increase in Reynolds number.

1. INTRODUCTION

The liquid crystal thermography (LCT) is a high resolution, non-intrusive optical technique for full field temperature visualisation and measurement, used successfully for the last decades on the surface having artificial roughness, in order to have details of Nusselt number distribution. The liquid crystals, is a material with state of matter between solid and liquid and thereby sharing properties of both solid and liquid [1]. The thermo-chromic liquid crystals possess a helical structure with a characteristic pitch length in the range of wavelength of visible light. The pitch length changes with application of temperature [2]. It reflects different colour depending on temperature when the surface is illuminated with white light source. The display colour is red at low temperature, green and blue at medium and high temperature respectively. A surface provided with artificial roughness is generally considered as an effective technique to enhance heat transfer from a heated wall. The presence of ribs over a surface generate wake zone before and behind the ribs, which deteriorates heat transfer [3]. Attaching the ribs on a surface require gluing, which became a resistance to heat transfer reducing effective heat transfer area. In order to overcome such types of difficulties, use of detached ribs may be an alternative method to enhance heat transfer. LCT is being used in the full extent for the visualisation and measurement of surface temperature distribution leading to convective heat transfer coefficients. Its advantage is that, this may cover the complete surface allowing global temperature distribution to be found. It is a non-intrusive, economic and capable of high spatial resolution and accuracy in temperature measurement. However, liquid crystal can be applied at relatively low temperature that means below 220 ºC, beside the temperature, there are certain other factors are in favour of LCT, are viewing angle, illumination system, image capture system, test section behaviour etc. Tanda [3] uses LCT to study the heat transfer of a rectangular channel roughened with repeated ribs. The roughened surface heated by isoflux heating having duct aspect ratio of five. The ribs cross section was rectangular or square, arranged as V-shaped in an angle of 45º or 60º with respect to main flow. The effect of broken ribs was also compared with that of continuous ribs. Tanda [4] in another study using LCT observed that the channel roughened with diamond shaped elements on one of its broad wall increases 4.4 times more heat transfer than that of smooth channel for equal mass flow rate. Cavallero et al. [5] carried out an experimental investigation in a rectangular channel with continuous and broken parallel rib roughness by means of LCT to investigate the heat transfer from the roughened surfaces. They observed that average heat transfer coefficient were 2 and 3 times more than that of smooth surface for continuous and broken ribs respectively. Wang et al. [6] studied the distribution of heat transfer using LCT over a surface having rib orientation transverse to the main stream with its cross section of square, equilateral triangle and trapezoidal. Result showed that highest heat transfer coefficient and friction factor occurred in trapezoidal ribs with decreasing height in flow direction and the reverse happened in trapezoidal ribs with increasing height in flow direction. It was also found that the characteristics of heat transfer and friction remain nearly equal for both square and triangular shaped ribs. Tariq et al. [7] using LCT performed an experimental study for flat and ribbed surfaces and observed that the local Nusselt number, average Nusselt number and skin friction coefficient of the roughened surface were more than the smooth surface. Ghorbani-Tari et al. [8] applying LCT under steady state condition made an experimental study to know heat transfer behaviour between the first two adjacent ribs in a straight rectangular channel. The ribs were continuous and transverse in flow direction attached to one side of the channel cross section and heated uniformly. The experimental parameters were rib pitch to height ratio values of 10, 20 and 30, where Reynolds number range was 57000 to 127000. The result revealed that the distance between reattachment point and the upstream rib edge is more at entrance region than this occurring at fully developed region in the flow field, when the ribs were positioned transversely in the channel flow.

It is clear from the literature that most of the studies of heat transfer related to attached ribs of various shapes and sizes are placed transverse to the flow direction on a heated surface having different cross section of channel. The detached square continuous ribs on an uniform heated surface of a rectangular channel placed transversely in flow direction has not been so far studied by using LCT according to author's knowledge. Hence it become worth noting to study about this. Considering all above, the objective of this study is measurement of heat transfer by using LCT varying relative roughness pitches and clearances of detached rib channel flow. The comparison of its thermal performance is also made with that of attached square ribs in similar operating condition.

2. EXPERIMENTAL SETUP

The schematic diagram of experimental setup is represented in Figure 1. It is an open loop induced flow air duct. The setup comprise of inlet section, test section, outlet section, an orifice-meter, control valve, flexible pipe and a blower. Air at ambient condition drawn through bell mouth entrance section and strainer to the inlet section of the rectangular duct, whose width (W) of 160 mm, height (H) of 40 mm and having hydraulic diameter (D_h) of 64 mm. The length of inlet section is 2 m ($31.25D_h$). The entire channel is made of 19 mm plywood. A digital micro manometer is used to determine the pressure difference across the test section. An aluminium plate of size of (700 mm x 160 mm x 3 mm) is used as roughened test section. The electric heater connected with a variac is used to provide uniform heat flux to the aluminium plate. A thin TLC (thermo-chromic liquid crystal) sheet is used over the test section to determine local wall temperature. The top frontal surface of the test section having plexi-glass wall to access images through CCD camera. The plexi-glass wall was covered by 20 mm polystyrene material to avoid heat loss to the ambient and removed at the time of optical access of the heated plate. The temperature of inlet and exit air is measured by T type thermocouples connected to a data logger. After the exit section baffles are provided for mixing of the air before recording its outlet temperature. A control valve followed by an orifice meter is connected before the blower to control the mass flow rate of the air through the duct. The mass flow rate of air is measured by an orifice meter connected with a digital manometer. In order to isolate the vibration from blower to the experimental setup a flexible pipe is used just before the blower suction. The discharge of blower is ducted out of the lab with help of flexible pipe to maintain constant temperature inside the lab. The pictorial view of the experimental setup is presented in Figure 2. Ribs are made of aluminium having square cross section (6 x 6) mm^2 detached from the heated aluminium plate with the help of small spacers and placed transversely to the flow direction. The ribs function is only to disturb the flow and the clearance generated by the position of the rib over the surface will produce turbulence at the vicinity of the wall, leads to enhance in heat transfer.

3. LIQUID CRYSTAL CALIBRATION

Any quantitative application of TLC (thermo-chromic liquid crystal) requires an accurate calibration to establish a colour-temperature relationship. In general TLC signal is quantified to hue, saturation and intensity. The variance of hue with temperature is less compared to intensity or saturation. The hue based image processing is defined in terms of RGB (red, green and blue). The colour images are recorded through a CCD camera, digitized to RGB format. The hue values increase monotonically with the TLC temperature.

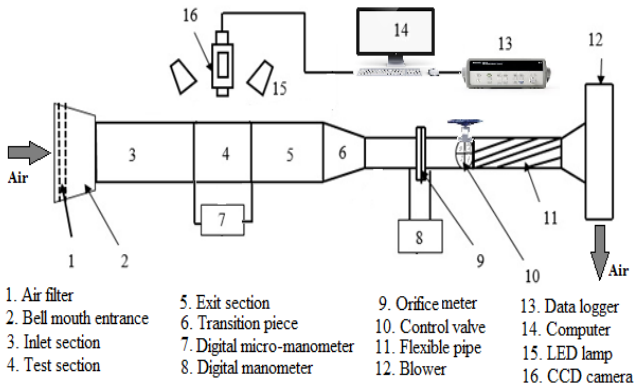

Figure 1. Schematic diagram of the experimental setup

Figure 2. Photograph of the experimental setup

3.1 Calibration test setup and procedure

The Figure 3 represents the schematic diagram of the test section, comprises of different layer such as 3 mm thickness aluminium plate, a heater and a layer of thermal insulation. A pre-packed TLC film of 0.15 mm thickness is used over the aluminium plate. The TLC film consists of a micro-encapsulated TLC layer coated on polyester (Mylar) film having a background colour with black ink, and backed with adhesive. The image acquisition system consists of a personal computer, a CCD camera (IMAGINGSOURCE, DFK 31AU03) and a light source. The TLC image was captured by a CCD camera having configuration of 1024 x 768 pixel resolution. The software "IC capture 2.3" interface was used to collect and store the data. The stored images in RGB format subsequently were processed by software (MATLAB R2014b) to get the hue value. Four LED lamps 35 watt each was used to illuminate the test section at the time of image capturing. In order to avoid IR heating of the test plate, the

LED light were switched on at the time of image acquisition only. The light source, LED lamps and CCD camera were mounted vertically to the supporting frames positioned directly above the test plate. To prevent the interference of surrounding light noise, the test section along with CCD camera, light source and illumination lighting were confined by black surroundings during experiment. The calibration experiment was performed maintaining identical parameters to optical arrangements as that of heat transfer experiments. The steady state method of calibration was followed for this study. This test was performed by slowly heating the aluminium plate whose top surface, covered with TLC film. The air temperature at the exit of the test section was measured with five numbers of T type thermocouple having accuracy of ± 0.1 ºC. The thermocouples were placed in small holes drilled on various locations over the plate with silver based paint and fixed in position by epoxy. In order to maintain isothermal condition in test section during the entire calibration test the inlet and outlet passage of test duct was blocked.

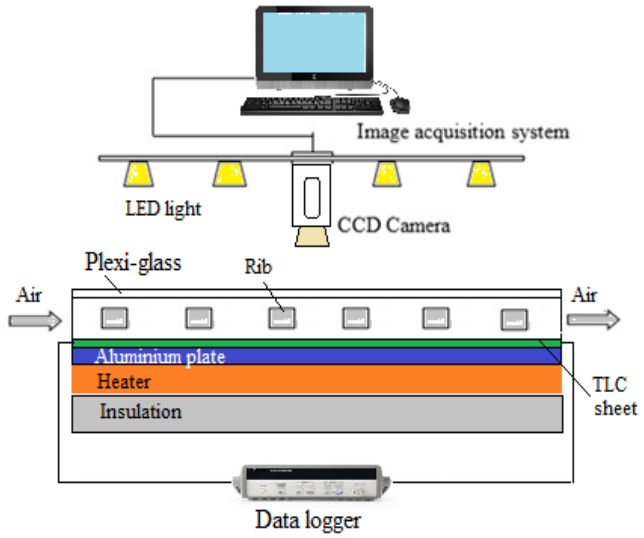

Figure 3. Schematic diagram of test section

3.2 Hue-temperature calibration curve

The typical behaviour of liquid crystal temperature with hue is observed from some sample regions of images of size (150 x 150) pixel each (from where thermocouples were attached at the test zone of aluminium plate) were extracted from the images of the calibration experiment. The spatial hue average for this region was used to construct a calibration curve. About 100-110 samples of images were collected for calibration curve. The wide band TLC sheet (R40C5W) used displays red colour at 40 ºC with a band width of 5 ºC. The increase in temperature of the crystal changes the colour to red, green and blue sequentially before turning black again. Figure 4 represents the relation between hue and temperature. The relationship obtained in polynomial form of degree two, as shown in Eq. (1).

$$T = 16.647H^2 + 17.379H + 38.82 \quad (1)$$

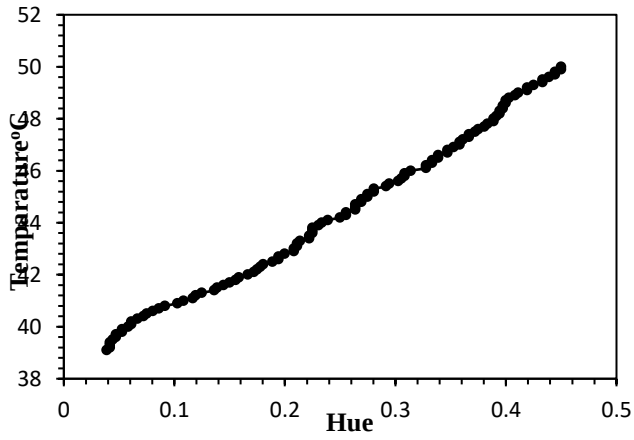

Figure 4. Hue-temperature calibration curve

4. EXPERIMENTAL PROCEDURE AND DATA REDUCTION

At steady state condition, the temperatures and TLC images were recorded and are transformed to a bmp file by the help of frame grabber. Software is used to convert the RGB values to HSI values pixel by pixel. Calibration curve is used to transform the hue values into the plate temperature and to get heat transfer coefficient, from the following relation.

$$h = \frac{q_{conv}}{(T_{LC} - T_b)} \quad (2)$$

where q_{conv} is the convective heat flux, T_{LC} is the plate temperature displayed by TLC and T_b is the bulk temperature of air at the x- position along the flow direction.

At a distance of x- the air bulk temperature is obtained by the following equation

$$T_b = T_{in} + \frac{(q_{conv}).A.(x/L)}{mc_p} \quad (3)$$

where T_{in} is the inlet temperature of air, m is the mass flow rate, c_p specific heat at constant pressure, L is the length of heated surface, A is the area exposed to air flow of the plate surface. The convective heat flux was calculated as

$$q_{con} = \frac{Q_{el} - Q_{rad} - Q_{dis}}{A} \quad (4)$$

where Q_{el} is the power supplied to heater ($V.I$), Q_{rad} is calculated radiative heat transfer to the surroundings, Q_{dis} is the heat dissipated through the insulation.

The Nusselt number (Nu) and Reynolds number (Re) are determined as

$$Nu = \frac{hD_h}{k}$$

$$\mathrm{Re} = \frac{GD_h}{\mu} \tag{5}$$

where k = thermal conductivity of air, μ = dynamic viscosity of air and G = mass velocity of air = (m / WH). The friction factor is obtained using pressure drop across the test section as:

$$f = \frac{2\Delta P_d D_h}{4\rho L V^2} \tag{6}$$

ΔP_d = pressure drop between two pressure taps
L = distance between two pressure taps
ρ = density of air
V = fluid velocity through the duct = m/ (ρWH).

5. EXPERIMENTAL UNCERTAINTY

In this study Moffat [9] proposed method of experimental uncertainty is used to perform analysis of uncertainty. The uncertainty results (based on with 95 % confidence level in normal distribution) in Nusselt number is calculated to be within ± 6.23 %. The uncertainty values in friction factor and Reynolds number are evaluated as ± 2.3 % and ± 2.24 % respectively.

6. RESULTS AND DISCUSSION

In order to verify the experimental reliability, a preliminary test has been performed on the similar condition on smooth duct and the obtained result has been compared with the literature available. The design and fabrication of experimental setup has been made by comparing with the previous work and also according to ASHRAE 93-77 standards. The details of setup presented in the section 2 of this study. A test zone along the test section of the setup has been used for LCT experimental work. The length of test zone is 320 mm and width of 140 mm. The test zone is placed from a distance of 192 mm (3 D_h) and 188 mm (2.9 D_h) from inlet and exit end respectively, along the central line of test section. The position of selection of test zone is such a way that the flow attains fully developed condition and non-influence of end effect of the test section of the duct.

6.1 Heat transfer coefficient for smooth duct

The Nusselt number over smooth surface obtained by liquid crystal thermography (LCT) technique have been compared with Dittus-Boelter Eq. (7), [10] for the span of Reynolds number 8000 to 22097.

$$Nu_s = 0.023\ \mathrm{Re}^{0.8}\ \mathrm{Pr}^{0.4} \tag{7}$$

where Nu_s = Nusselt number of smooth surface, Pr = Prandtl number.

Figure 5, depict the measured heat transfer coefficient are in good agreement with the value of Eq. (7) with a slight deviation. It can be seen that the increase in Reynolds number reduces the deviation between them. The reason for this may be the conduction effect in very low finite thickness heated plate, when ribs are used the heat transfer coefficient became higher than the smooth plate and this problem tends to eliminate. Figure 6 shows maps of Nusselt number in smooth duct at Re = 22097, where it appears almost green in colour, that means the liquid crystal sheet in second phase of its colour zone of RGB.

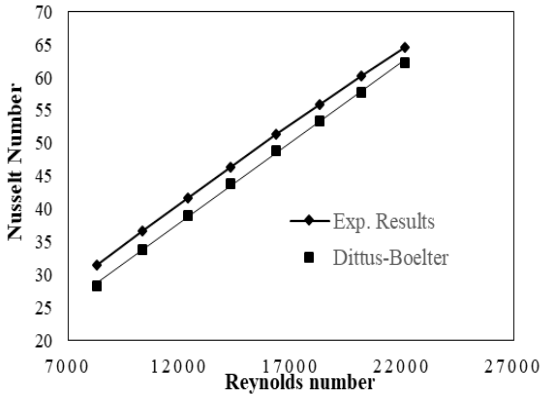

Figure 5. Nusselt number as a function of Reynolds number for smooth duct

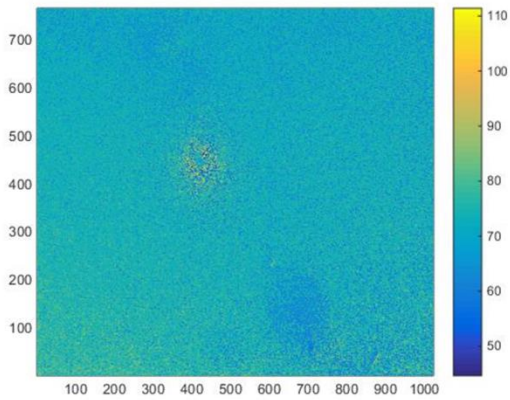

Figure 6. Nusselt number distribution over smooth surface (Re = 22097)

6.2 Heat transfer in detached rib ducts

Repeated ribs are often used to increase heat transfer in heat exchange systems, but existence of solid attach ribs on the heated surface deteriorate heat transfer immediately behind the ribs, due to the generation of wake zone. This problem can be overcome by the application of detached ribs over the surface.

6.2.1 Effect of relative roughness pitch

The Figure 7 depicts the variation of Nusselt number influenced by relative roughness pitch. The heat transfer increases from P/e = 7 to 9 and thereafter it decreases from 9 to 11. This can be accomplished that it attains an optimum value at P/e = 9. The reason for this may be due to displacing a small distance of the rib from heated plate, it generates wall jets. The wall jets issuing between rib and the heated wall moves towards downstream and expanded towards its core

flow. Part of the wall jet fluid meet the fluid stream flows over the rib top surface rear corner at the wakes. The shear layers generated by these two streams with different velocities and temperature, sheds vortices and subsequently grows and sheds to downstream until the front edge of the next rib. Furthermore, the fluid steam spilt into two halves and flows over and beneath the rib. The value of relative roughness pitch changes the formation of vortex position between two adjacent ribs. The relative roughness pitch of less than the value of 9, decreases the frequency of shedding of vortices, and decreases the heat transfer. The relative roughness pitch values of higher than 9, decreases the mixing of the flows over and below the ribs, causes the lower heat transfer. The aforementioned phenomenon takes place at *P*/*e* = 9, the condition below and above than 9 does not generate the similar event as that of *P*/*e* = 9 which leads to low heat transfer at *P*/*e* values of 7, 8, 10 and 11.

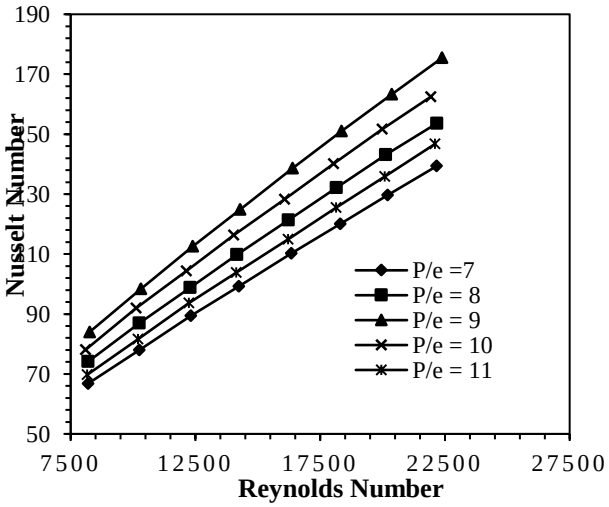

Figure 7. Nusselt number as a function of relative roughness pitch

6.2.2 Effect of clearance ratio

The Figure 8 shows the variation of Nusselt number influence by clearance ratios (*C*/*e*). The trend is similar to that of relative roughness pitch. It seems that the fluid flows through the smaller gap between plate and rib produces high velocity jet at downstream of the rib, that means the gap plays the role of a nozzle as contraction and expansion of flow takes place just before, after and beneath the rib. The accelerated fluid through gap between the rib base and heated plate carried plenty of heat from the heated surface below the rib and get mixed to core flows. This produces low temperature gradient between heated wall and rib base. Hence it reduces in heat transfer at rib top and back face of the rib. On the other hand the wake zone behind the detach rib tends to restrain the wall jet to spreading up to a certain distance at the downstream of the rib. Thereafter wall jet shear layer and the associated turbulent transport enhancement phenomena remain active adjacent to heated wall for the central and later part of the inter rib region, which enhances heat transfer. Clearance below than the certain value does not act like a nozzle means less amount of mass flow, that tends to low heat transfer at lower clearance ratio. Similarly, when clearance ratio became more than the certain value, increases the mass flow but makes the acceleration low through the gap, leads to weak in turbulence in the downstream of the rib, that reduce in heat transfer. The maxima in heat transfer occur at *C*/*e* = 0.47 and decreases with on the other hand lower heat transfer occurs for the remaining clearance ratios.

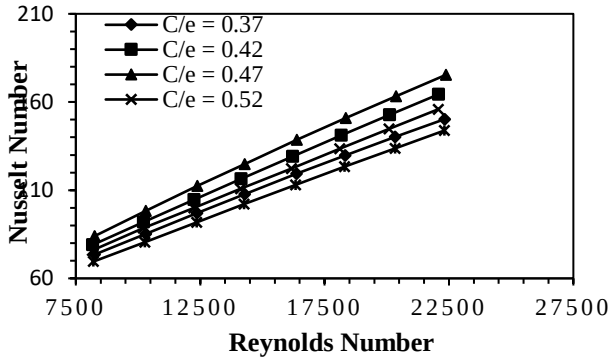

Figure 8. Nusselt number as a function of clearance ratio

7. PERFORMANCE EVALUATION

It is worth noting to know the performance of this roughened surface before its application in any heat exchanger. The rectangular channel having uniform heating on one broad wall with detached rib roughness and remaining other three walls are insulated, this condition is resemblance to a solar air heater. The performance of a roughened solar air heater can be judged with reference to smooth surface, considering geometric and operating parameters proposed by Bergles et al. [11]. The augmentation in heat transfer can be obtained either maintaining constant mass flow rate or fixing the pumping power requirement of a roughened surface to that of a smooth surface. The heat transfer for the roughened surface is evaluated and that for the smooth surface is obtained from Eq. (7). Similarly for friction factor, it can be compared with the Blasius Eq. (8) [12]; and is given as;

$$f_s = 0.085\,\mathrm{Re}^{-0.25} \tag{8}$$

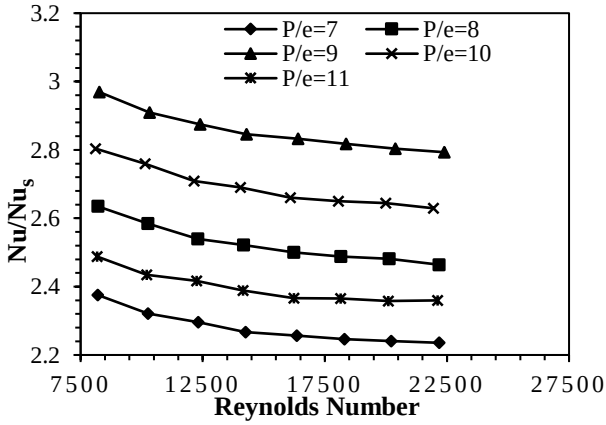

Figure 9. Nusselt number ratio as a function of relative roughness pitch

The degrees of heat transfer augmentation expressed as the ratio of heat transfer of roughened surface (Nu) to that of heat transfer over smooth surface (Nu_s) is represented by (Nu/Nu_s). The Nusselt number ratio as a function of relative roughness pitch and Reynolds number is plotted in Figure 9. It indicates

that performance decreases with increase of Reynolds number and highest performance observed at P/e = 9 at low Reynolds number and lowest performance at P/e = 7 at highest Reynolds number, when clearance ratio is 0.47 and aspect ratio is 4. Hence for best performance it should be run at low flow rate at P/e = 9, C/e = 0.47 and W/H = 4, considering heat transfer only. The Figure 10 shows the Nusselt number distribution having detached rib at P/e = 9, C/e = 0.47 and W/H = 4. It reveals that, there is mixture of dark green and yellow colour near the rear concave corner of the rib, indicate more heat transfer than blue colour region. This means that no hot spot at the downstream of rib, as flow takes place from left to right.

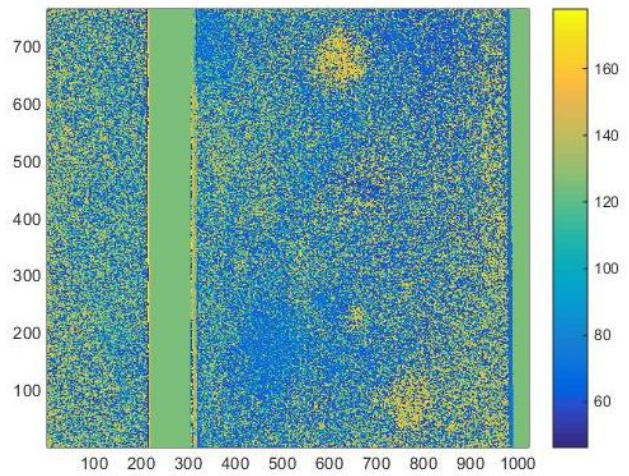

Figure 10. Nusselt number distribution for detach rib (Re = 18358, C/e = 0.47and P/e = 9)

8. COMPARISON OF DETACH RIB WITH ATTACHED RIB

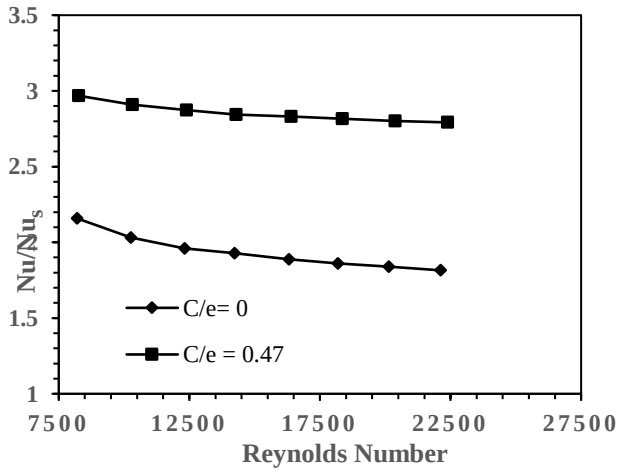

Figure 11. Comparison of enhancement ratio of detached rib with attached rib

The Figure 11 illustrate the comparison of enhancement ratio of heat transfer of attached rib (C/e = 0) with that of detached ribs (C/e = 0.47) at P/e = 9 and W/H = 4. It clearly indicates that detach rib perform better than the attach rib for the entire Reynolds number studied. The enhancement ratio of both attach and detach ribs reduces with increase in Reynolds number. Similarly the friction factor ratio of attached rib is compared with detached rib at P/e = 9 and W/H = 4 is presented in Figure 12. It reveals that the ratios increase with decrease in Reynolds number. It is also found that the friction factor ratio is more in case of detach rib than in attach rib for the entire Reynolds number. This can be explained as the detached ribs protrude much to the core flow creates more turbulence and friction factor.

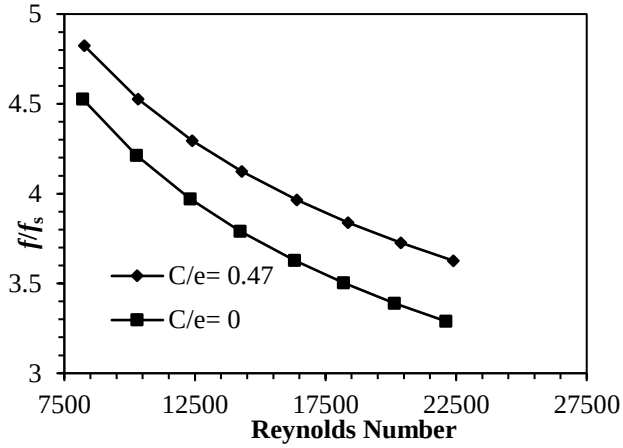

Figure 12. Comparison of friction factor ratios of detached rib with attach rib

In order to have a clear idea of improvement in performance of the detached rib surface compared to that of attached rib, considering heat transfer along with friction, the thermal performance parameter Eq. (9), [12] is plotted as a function of Reynolds number in Figure 13. The thermal performance parameter may be defined as;

$$TPP = \frac{Nu / Nu_s}{\left(f / f_s \right)^{1/3}} \tag{9}$$

It can be observed from Figure 13 that the thermal performance parameter is higher in detached rib than that of the attached rib for the entire Reynolds number studied. Furthermore it may be observed that increase in Reynolds number increases thermal performance parameter of detached rib.

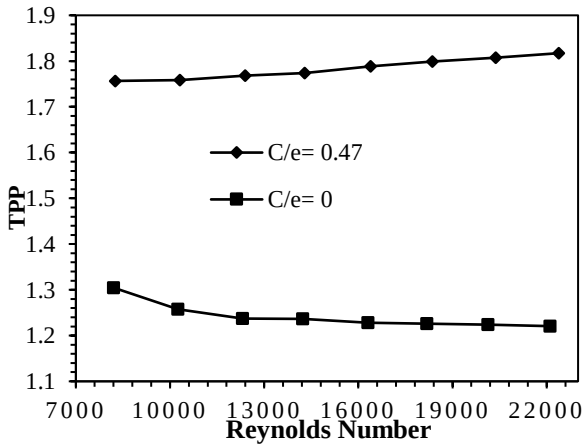

Figure 13. Comparison of thermal performance parameters for attached and detached ribs

9. CONCLUSIONS

In this study liquid crystal thermography technique has been used in heat transfer measurement of an artificially roughened surface having detached rib with varying relative roughness pitch (*P*/*e)*, clearance ratio (*C*/*e*) and Reynolds number (Re) where aspect ratio (*W*/*H*) of the duct is kept constant. Based on the study the following observations are made;

- The increases in relative roughness pitch increases Nusselt number from *P*/*e* value of 7 to 9 and thereafter decreases from *P*/*e* value of 9 to 11.
- The increase in clearance ratio increases Nusselt number from *C*/*e* value of 0.37 to 0.47 and thereafter decreases from *C*/*e* value of 0.47 to 0.57.
- Nusselt number attains its maxima value at *P*/*e* = 9 and *C*/*e* = 0.47.
- Friction factor ratios increase with decrease in Reynolds number for attached and detached rib.
- Thermal performance of detached rib is better than attached ribs in all flow rates.
- Optimum thermal performance obtained at *P*/*e* = 9, *C*/*e* = 0.47 and in high Reynolds number.

ACKNOWLEDGEMENTS

The authors wish to thanks to the DST, Govt. of India for funding and supporting to carry out this project Ref. SERB - DST Grant: SB/EMEQ-314/2013; dated: 08/07/2013.

REFERENCES

[1] Wang L, Sunden B, Wang C. (2014). Temperature measurement in Heat Transfer. Course MVK 115 Project Energy Technology, Lund University, Lund, Sweden.

[2] Stasiek J, Wierzbowski M, Klosowicz S, Zmija J, Collins MW. (2002). Liquid crystal thermography for technical and biomedical application, WIT Press, UK.

[3] Tanda G. (2004). Heat transfer in rectangular channels with transverse and V-shaped broken ribs, International Journal of Heat and Mass Transfer 47: 229-243. https://doi.org/10.1016/S0017-9310(03)00414-9

[4] Tanda G. (2001). Heat transfer and pressure drop in a rectangular channels with diamond-shaped elements. International Journal of Heat and Mass Transfer 44: 3529-3541. https://doi.org/PH: S0017-9310(01)00018-7

[5] Cavallero D, Tanda G. (2002). An experimental investigation of forced convection heat transfer in channels with rib turbulators by means of liquid crystal thermography. Experimental Thermal and Fluid Science 26: 115-121. https://doi.org/PH: S0894-1777(02)00117-6

[6] Wang L, Sunden B. (2007). Experimental investigation of local heat transfer in a square duct with various shaped ribs. Heat Mass Transfer 43: 759-766. https://doi.org/10.1007/S00231-006-0190-Y

[7] Tariq A, Swain SK, Panigrahi PK. (2002). An experimental study of convective heat transfer from flat and ribbed surfaces. Indian Journal of Engineering and Material Science 9: 464-471.

[8] Ghorbani-Tari Z, Sunden B. (2012). Experimental study of convective transfer in the entrance region of a rectangular duct with transverse ribs, Proceedings of the ASME 2012 Summer Heat Transfer Conference HT2012, Rio Grande, Puerto Rico.

[9] Moffat RJ. (1988). Describing the uncertainty in experimental results. Experimental Thermal Fluid Science 1: 3-17.

[10] Forced convection internal flow in ducts (1980), IV edition, McGraw Hill, New York.

[11] Bergles AE., Blumenkrantz, AR, Taborek J. (1974). Performance evaluation criteria for selection of enhanced heat transfer surfaces. Proceedings of the 5th Heat Transfer Conference, Tokyo, Japan 2: 239-243.

[12] Hand Book of single phase convective heat transfer (2003). John Wiley, New York.Unsteady MHD free convection flow of Casson fluid past over an oscillating vertical plate embedded in a porous medium. Engineering Science and Technology, an International Journal 18(3): 309-317, 2015.

[13] Kataria HR. Patel HR. (2016). Radiation and chemical reaction effects on MHD Casson fluid flow past an oscillating vertical plate embedded in porous medium. Alexandria Engineering Journal 55: 583-595.

[14] Hussanan MZ. Salleh, Khan I, Tahar RM. (2017). Heat transfer in magnetohydrodynamic flow of a Casson fluid with porous medium and Newtonian heating. Journal of Nanofluids 6(4): 784-793.

NOMENCLATURE

A	area of roughened plate, m^2
C	clearance between rib and plate, m
C/e	clearance ratio
c_p	specific heat, $J.kg^{-1}.K^{-1}$
D_h	hydraulic diameter, m
e	rib height, m
f	friction factor
G	mass velocity of air
h	convective heat transfer coefficient
H	duct depth, m
k	thermal conductivity, $W.m^{-1}.K^{-1}$
L	length of test plate, distance between two pressures taps, m.
m	mass flow rate, $kg.s^{-1}$
Nu	Nusselt number
P	rib pitch, m
Pr	Prandtl number
P/e	relative roughness pitch
q_{con}	convective heat flux, $W.m^{-2}$
Q_{dis}	heat dissipated through insulation, W
Q_{el}	measure power of heater, W
Q_{rad}	radiative heat transfer rate, W
Re	Reynolds number
TPP	thermal performance parameter
T_b	bulk temperature of air, ^oC
T_{in}	inlet air temperature, ^oC
T_{LC}	surface temperature detected by TLC, ^oC
W	width of duct, m
W/H	aspect ratio

Greek symbols

Δ difference
μ dynamic viscosity of air, Pa.s
ρ density of air, $kg.m^{-3}$

Subscript

h hydraulic
s smooth surface